Ulmeanu, M., Grubb, M. P., Jipa, F., Quignon, B., & Ashfold, M. N. R. (2015). 3-D patterning of silicon by laser-initiated, liquid-assisted colloidal (LILAC) lithography. Journal of Colloid and Interface Science, 447, 258-262. https://doi.org/10.1016/j.jcis.2014.11.001

3-D patterning of silicon by laser-initiated, liquid-assisted colloidal (LILAC) lithography

M. Ulmeanu[1*], M.P. Grubb[1], F. Jipa[2], B. Quignon[1] and M.N.R. Ashfold[1]

[1]School of Chemistry, University of Bristol, Cantock's Close, Bristol BS8 1TS, UK

[2]National Institute for Laser, Plasma and Radiation Physics, Laser Department, Magurele 077125, Romania

Abstract: We report a comprehensive study of laser-initiated, liquid-assisted colloidal (LILAC) lithography, and illustrate its utility in patterning silicon substrates. The method combines single shot laser irradiation (frequency doubled Ti-sapphire laser, 50 fs pulse duration, 400 nm wavelength) and medium-tuned optical near-field effects around arrays of silica colloidal particles to achieve 3-D surface patterning of silicon. A monolayer (or multilayers) of hexagonal close packed silica colloidal particles act as a mask and offer a route to liquid-tuned optical near field enhancement effects. The resulting patterns are shown to depend on the difference in refractive index of the colloidal particles ($n_{colloid}$) and the liquid (n_{liquid}) in which they are immersed. Two different topographies are demonstrated experimentally: a) arrays of bumps, centred beneath the original colloidal particles, when using liquids with $n_{liquid} < n_{colloid}$, and b) a combination of holes, created in the interstices between the colloidal particles, and bumps when using liquids with $n_{liquid} > n_{colloid}$ – and explained with the aid of complementary Mie scattering simulations. The LILAC lithography technique has potential for rapid, large area, organised 3-D patterning of silicon (and related) substrates.

* Corresponding author Phone: + 44 (0) 1179288312, Fax: + 44 (0) 1179277985

E-mail: magdalena.ulmeanu@bristol.ac.uk

Introduction

The search for new and improved large area nanopatterning techniques for silicon (Si) and other semiconductor materials is a subject of intense investigation due to the many envisaged technological applications of such surfaces. Surface nanopatterning can be achieved in a number of ways – *e.g.* ion and e-beam lithography [1], dip pen lithography using the tip of an atomic force microscope [2], localized excimer-laser irradiation [3] or by using the near-field effects induced by laser irradiating microsphere-covered substrates in air [4] or in a liquid medium [5]. A layer of microspheres directly on the surface acts as an array of near-field lenses that focusses the incident radiation into a multitude of spots, thereby inducing formation of an organized array of nanostructures in a single step.

We have previously shown that the medium-tuned optical field enhancement around self-assembled silica colloidal particles irradiated with a fs or ps pulse of laser radiation can be used to fabricate periodic arrays of micro/nanostructures on semiconductor substrates [6]. Specifically, we showed that laser processing under methanol and carbon tetrachloride influenced the patterning of both Si and GaAs substrates, but this earlier study left open the question as to whether it was the composition of the liquid, or its refractive index, (or both), that was responsible for the obtained patterns.

The structuring of Si is of particular interest given its predominance in electronic devices. Hence the great current interest in understanding the physical processes involved in the formation of Si tips [7,8], pores [9] and through-holes in bulk Si [10]. Direct laser micro/nanostructuring employing a colloidal mask could constitute a relatively straightforward and cost-effective technology for patterning Si substrates. Here we present extensive, detailed experimental demonstrations of the formation of uniform areas of bumps and holes on Si using a laser-initiated, liquid-assisted colloidal (LILAC) lithography technique with no fewer than six different liquids. The Si structuring is described in terms of medium-tuned optical field enhancement effects around self-assembled silica colloidal particle layers irradiated with the frequency doubled output of an ultrafast Ti-sapphire laser. The choice of liquid medium is shown to have a profound influence on the optical field enhancement and thus on the eventual surface patterning. The chosen liquids clearly partition into two classes: i) methanol, acetonitrile and n-hexane, each of which has a refractive index (n_{liquid}) less than that of the colloidal particle ($n_{colloid}$) and ii) chloroform, carbon tetrachloride

and toluene, for which $n_{liquid} > n_{colloid}$. Mie theory modelling of the optical near-field effects around colloidal particles immersed in a liquid medium identifies three different factors that affect the surface structuring: a) variations in the effective focal length, which influences the depth at which energy couples into the substrate, b) enhanced near fields immediately under the colloidal particles when $n_{liquid} < n_{colloid}$ and c) enhanced near fields between the colloidal particles when $n_{liquid} > n_{colloid}$.

The present studies represent a significant step forward in understanding, modelling, and predicting the detailed patterning of Si substrates using medium tuned optical field enhancement effects. We anticipate that further developments and applications of the LILAC technique will provide a deeper mechanistic understanding of this new route to nano- (micro-) structuring surfaces with user controllable density distributions, topography and chemical surface composition, and foresee exciting potential applications in, for example, tissue engineering and sensors.

Materials and methods

All chemical materials in this study were obtained commercially and used as supplied. Aqueous suspensions of monodisperse (coefficient of variation (CV) of 10-15%) silica colloidal particles with mean radius R = 1.5 μm or 350 nm (10% solid concentration, with specified $n_{colloid}$ in the range 1.43-1.46 measured at λ = 589 nm) were sourced from Bangs Laboratories. The two steps of the LILAC lithography process are depicted in Figure 1.

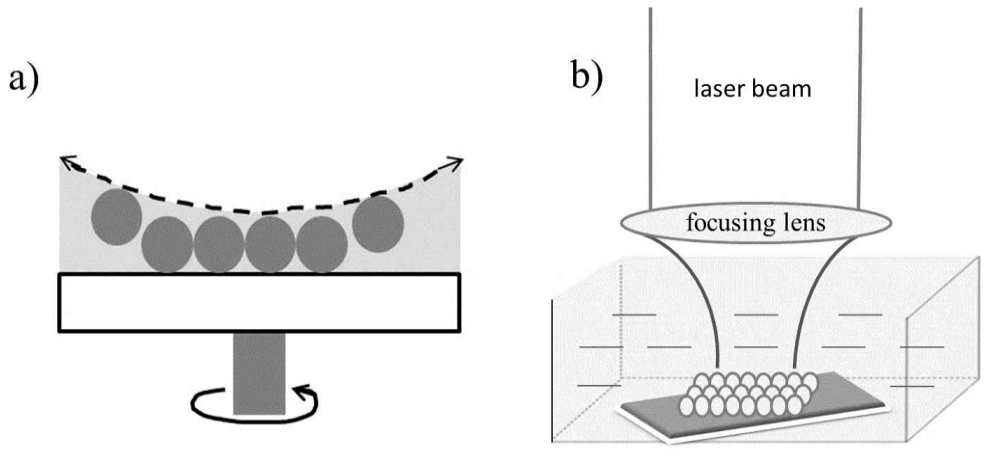

Figure 1. *Schematic representation of the two steps involved in laser-initiated, liquid-assisted colloidal lithography: a) deposition of a close packed array of colloidal particles on a Si substrate and b) liquid-assisted, laser irradiation of a selected area of the Si surface beneath the colloidal particle array.*

A close-packed monolayer (or multilayer) of colloidal nanoparticles was first fabricated by spin coating on an n-type Si substrate (Crystal GmbH), that had previously been treated in an oxygen plasma (Femto Diener, 80 W power, 0.5 mbar O_2 pressure) for 10 min to remove contaminants and render the surface hydrophilic. 500-700 μl aliquots of the colloidal silica in water suspension were dropped onto the 15 x 15 mm^2 Si substrates and left for ~1 min prior to spin-coating at speeds in the range 200-2500 revs s^{-1} for 2 minutes. The colloid coated substrate was then completely immersed in the liquid of interest (volume ~1 cm^3) in an open trough (dimension 25 x 25 x 20 mm^3) mounted on a motorised 2- (*X*,*Y*-) axis translation stage.

Selected area patterning was achieved using single 50 fs pulses of frequency doubled (400 nm) radiation from a Ti-sapphire laser (Coherent Vitara-S oscillator, Legend Elite HE+ regenerative amplifier and OPerA Solo optical parametric amplifier, operating at 1 kHz). Every 60^{th} pulse was selected from the kHz pulse train using a synchronized chopper wheel, directed from the horizontal to vertical using a turning mirror and then focused onto the sample with a plano-convex UV grade fused silica lens (250 mm focal length). The focal point – both in air and in the liquid of interest [11] – was established by test exposures prior to patterning. The typical spot size on the sample was ~50 μm in diameter, yielding incident laser fluences F_{laser} in the range 0.02-0.2 mJ cm^{-2}. Use of a sample translation speed ~ 2.5 mm s^{-1} ensured that each laser pulse interacted with a fresh sample area. Post irradiation, the samples were removed from the liquid, left to dry in air and characterized by scanning electron microscopy (SEM) and atomic force microscopy (AFM).

Results and Discussion

i) Mie theory simulations

Mie theory modelling was undertaken to illustrate how a liquid medium can affect the focusing properties and the near-field intensity distribution around a single colloidal particle. Mie's 1908 paper [12] first outlined how light scattering by small spherical particles can be

computed using Maxwell's electromagnetic theory [13]. Here, we have undertaken numerical Mie theory analysis using the FullWAVE 9.1 software (RSoft Design Group). The algorithm to model the optical near field around a single particle uses finite-difference-time-domain (FDTD) methods to solve Maxwell's curl equations as a function of discrete time and space. The simulation model comprises a silica colloidal particle (R =1.5 μm, $n_{colloid}$ = 1.44) placed in air (n = 1) or immersed in a liquid medium with refractive index n_{liquid} in the range 1.35-1.50, and linearly polarised (along Y) laser radiation (wavelength, λ = 400 nm) propagating in the Z-direction. Figure 2 illustrates the magnitude of the Poynting vector $|S_z|$ calculated for media with different n_{liquid}. $|S_z|$ represents the directional energy flux per unit area in the vicinity of the colloidal particle. The focal point for the R = 1.5 μm colloidal particle in air is located at Z/R = 1.2 (*i.e.* close beyond the surface of the particle, fig. 2(a)). The field enhancement decays near exponentially with increasing Z indicating that, for efficient patterning, the surface of the particle should be in the near-field region.

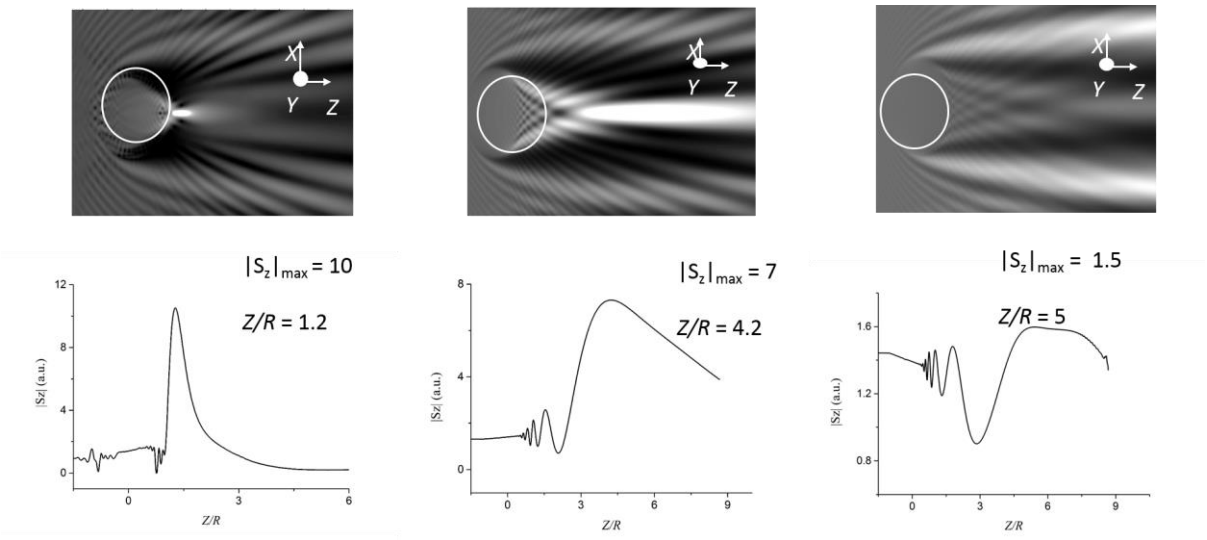

***Figure 2**. False grey scale plots (above) and cross-sectional views (along Z, at X = 0, below) illustrating the magnitude of the Poynting vector $|S_z|$ in the vicinity of an isolated R = 1.5 μm silica particle ($n_{colloid}$ = 1.44, illustrated by the open white circle) immersed in media with refractive index n = a) 1.0, b) 1.35 and c) 1.49. The incident laser beam (λ = 400 nm) is linearly polarized along the Y axis and propagates in the Z direction.*

More generally, the present simulations identify two distinct regimes: (i) $n_{liquid} < n_{colloid}$ and (ii) $n_{liquid} > n_{colloid}$. In case (i), the peak $|S_z|$ remains on axis (*i.e.* X (and Y) = 0), and the field enhancement extends to much greater Z. For example, immersing the R = 1.5 μm silica particle in a medium with n_{liquid} = 1.35 extends the focal length from Z/R = 1.2 (in air) to Z/R = 4.2 (fig. 2(b)). The extension of focal length predicted by use of a colloidal particle

immersed in a liquid with n_{liquid} slightly smaller than $n_{colloid}$ could offer a route to enhanced energy coupling deeper within the substrate [5]. Conversely, when $n_{liquid} > n_{colloid}$ (case (ii)), the largest field enhancements are predicted at the 'edges' of the colloidal particle (fig. 2(c)).

Figure 3 shows model results for the case of four silica particles aligned in a row along *X* on a Si substrate (n_{Si} = 5.56 at λ = 400 nm [14]) in two different model liquids. As before, the incident beam has a wavelength λ = 400 nm, is polarized along *Y* and propagates in the *Z* direction. The regions of peak absorbance in the case that $n_{liquid} < n_{colloid}$ are again predicted to occur beneath each particle (fig. 3(a)), while for the $n_{liquid} > n_{colloid}$ regime, maximum absorption is found in the interstices between the particles (fig. 3(b)). Absorption in these calculations is defined as the power absorbed within the spatial domain defined for the simulations, and the values shown in fig. 3 are those calculated at the substrate surface. These four particle simulations do not reveal any influence of near field interactions between neighbouring particles.

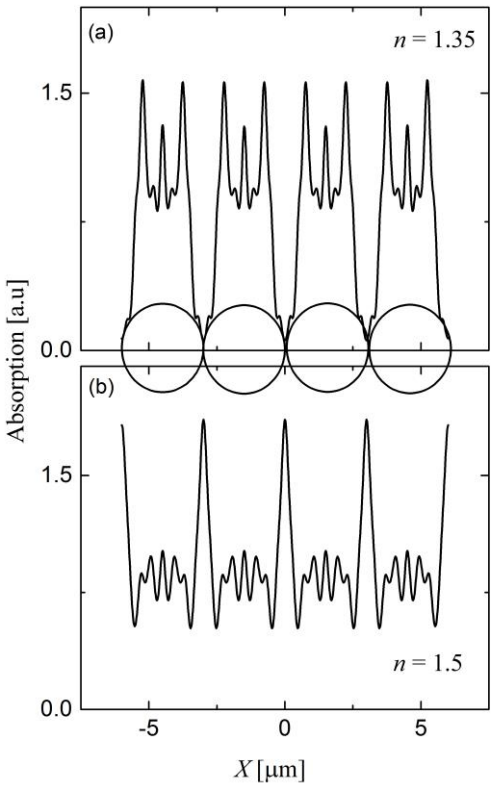

Figure 3. *Cross-sectional view of the predicted absorption at the surface of a Si substrate located beneath a line (along X) of four silica colloidal particles immersed in a liquid with (a)* $n_{liquid} < n_{colloid}$ *and (b)* $n_{liquid} > n_{colloid}$.

ii) Experimental studies

Nanopatterning of the surface of a silicon substrate by LILAC lithography was investigated using each of the liquids listed in Table 1. All are transparent to the 400 nm laser wavelength but, as reported previously [15], a liquid confined plasma is observable at the laser focal spot during irradiation.

Liquid	**Chemical formula**	**Refractive index (*n*)**
Methanol	CH_3OH	1.33
Acetonitrile	CH_3CN	1.34
n-Hexane	C_6H_{14}	1.37
Chloroform	$CHCl_3$	1.44
Carbon tetrachloride	CCl_4	1.46
Toluene	$C_6H_5CH_3$	1.49

Table 1. *Liquids used in the present LILAC lithography studies, together with their respective chemical formulae and refractive indices (measured at λ = 589 nm).*

Figure 4 shows a selection of top-view SEM images that illustrate the potential of LILAC lithography. The Si substrate in each case was covered with a monolayer of R = 1.5 μm silica colloidal particles. The low resolution image (panel (a)) shows a sequence of processed areas, each of which is the result of a single shot exposure. As reported previously, the colloidal particles in the irradiated area are efficiently removed – a process termed 'dry laser cleaning' [16]. The other panels show higher resolution views of (b) an unirradiated region of the hexagonal closed packed (hcp) monolayer and selected areas of Si substrates after single shot laser processing in (c) air, (d) CH_3OH, (e) n-C_6H_{14}, (f) CCl_4 and (g) $C_6H_5CH_3$.

These latter images illustrate the regularity of the 2-D patterning of the Si substrate achieved using the LILAC lithography technique, and the obvious change in the patterning depending upon whether n_{liquid} is less than, *i.e.* panels (d) and (e), or greater than, *i.e.* panels (f) and (g), $n_{colloid}$. The features in panels (d) and (e) were formed by single shot irradiation with F_{laser} ~0.1 mJ cm^{-2}, and are centred directly beneath the original positions of the colloidal particles

in the hcp monolayer on the Si surface. As panels (f) and (g) illustrate, the detail of the nanostructuring is very different in the case that $n_{liquid} > n_{colloid}$. These samples, prepared by single pulse laser processing with F_{laser} ~0.2 mJ cm^{-2}, show clear features in the interstices between the original colloidal particles and weaker features directly under the site of each particle.

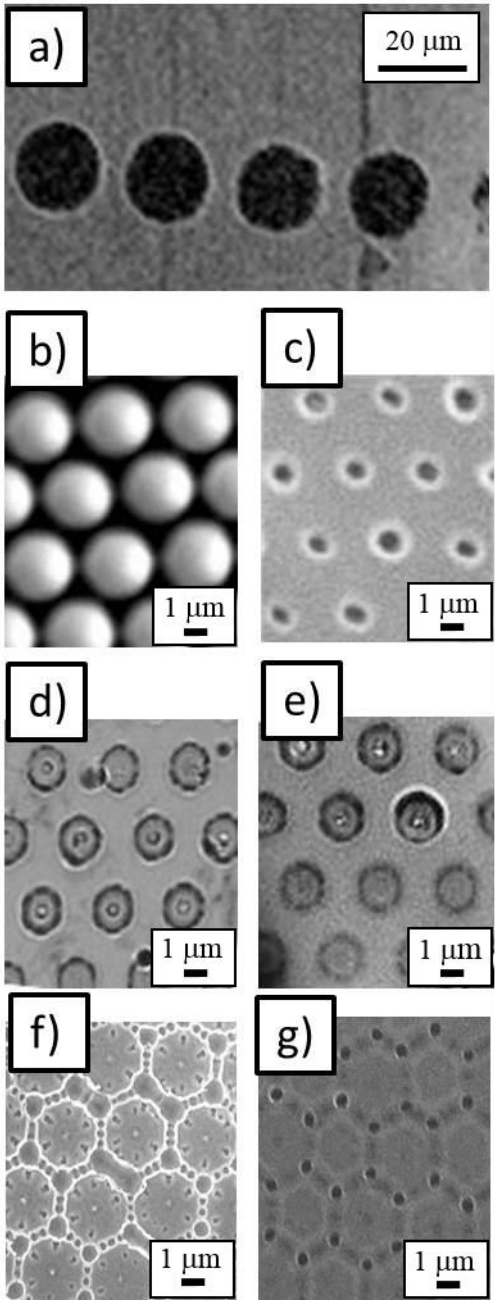

Figure 4. *SEM images showing (a) a Si substrate covered with a monolayer of R = 1.5 μm silica colloidal particles after LILAC lithography treatment, (b) an unirradiated region of the monolayer covered surface, and detailed views of the Si surface after single shot laser processing in (c) air (n = 1), (d) CH_3OH (n = 1.33),(e) n-C_6H_{14} (n = 1.37), (f) CCl_4 (n = 1.46) and (g) $C_6H_5CH_3$ (n = 1.49).*

Tilt-view SEM images show that the features obtained when $n_{liquid} < n_{colloid}$ (panels (d) and (e)) are bumps, as are the faint central features in the patterns formed with $n_{liquid} > n_{colloid}$ (panels (f) and (g)), while the more pronounced interstitial features in the latter are 'lipped' holes. This is confirmed by the line scan AFM measurements of features obtained by LILAC lithography through a monolayer of R = 1.5 μm particles shown in figs. 5(a) and 5(b). The former, created by processing in CH_3OH, shows a bump with a basal width of ~1.3 μm and peak height ~100 nm surrounded by a shallow moat. The features formed in the interstititial spaces between the colloidal particles when $n_{liquid} > n_{colloid}$, in contrast, are holes (~400 nm wide and ~100 nm deep) with raised rims – as shown in fig. 5(b) for the case of a Si sample processed in CCl_4.

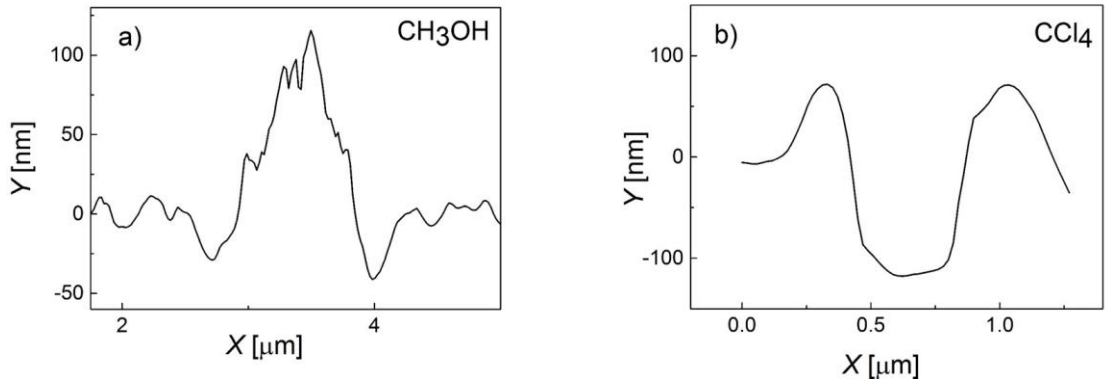

Figure 5. *Line scan AFM traces of features formed by LILAC lithography of a Si substrate using an array of R = 1.5 μm colloidal particles: (a) a bump formed in CH_3OH and (b) a lipped hole formed in CCl_4.*

The specific causes of bump and hole formation remain the subject of ongoing studies, but we note that the bumps have a very similar topology to that reported previously in the case of ns laser processing of Si through a colloidal mask in air (albeit at much higher incident fluences). Bump formation in that case was ascribed to localized melting and, since the density of liquid silicon is higher than that of the crystalline solid, a temporary depression of the surface. The melt zone cools from the outside inwards, the re-expansion that accompanies solidification squeezes the remaining liquid material in the core of the melt zone, and this compression is relieved by vertical expansion – thereby yielding a localised bump [17,18]. Such a mechanism, though appealing, is seemingly unable to explain the obvious hole formation in the case of fs LILAC lithography when $n_{liquid} > n_{colloid}$. What the present studies do show is that varying the refractive index difference $\Delta n = (n_{liquid} - n_{colloid})$ across the small

range –0.09 to +0.06 is sufficient to induce a striking change in the Si surface patterning; planned future studies will explore the generality of this behaviour, over a wider range of Δn space.

The variation and extension of the effective focal length when using a liquid with $n_{liquid} < n_{colloid}$ allows fabrication of patterns using multi-layered colloidal particle arrays. Figure 6 shows (a) low and (b) higher resolution 60° tilt view SEM images of a patterned Si substrate subjected to single shot LILAC lithography through a double layer of R = 350 nm colloidal particles immersed in CH_3OH. Formation of bumps with a base diameter ~300 nm and peak height ~100 nm is clearly evident, as are surrounding areas of mild ablation and what appears to be hairline cracks (arrowed in panel (b)) which we regard as a possible sign of processing induced tension in the Si surface.

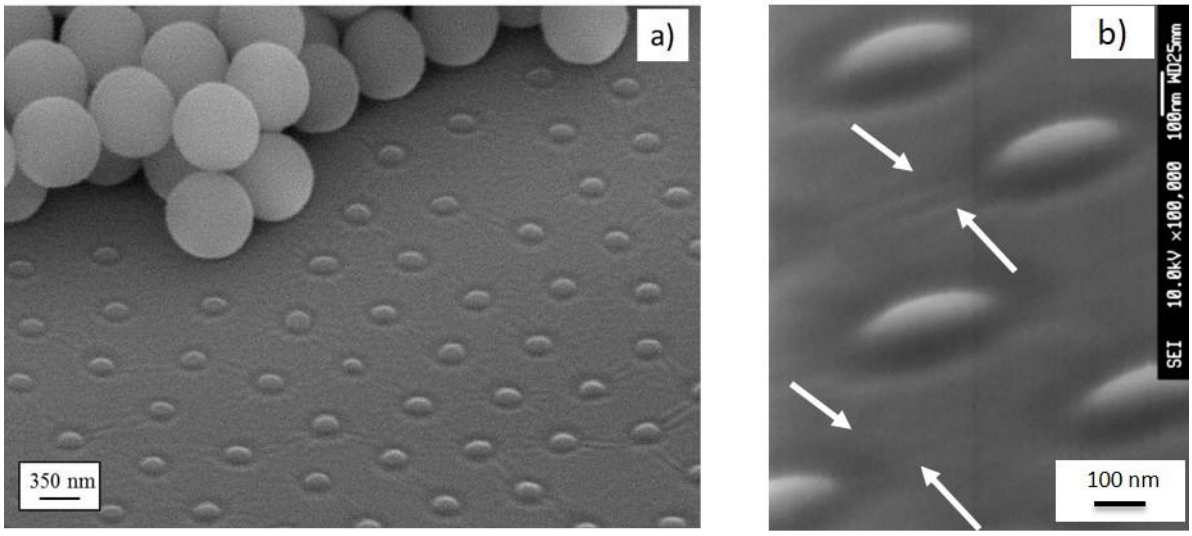

Figure 6. *a) Overview and b) detail 60° tilt view SEM images showing the surface pattern achieved on Si by single shot LILAC lithography using a double layer of R = 350 nm colloidal particles in CH_3OH, together with remaining particles at the periphery of the processed zone. Apparent hairline cracks are highlighted by arrows in b).*

FDTD analysis of multi-layer colloidal particle arrays has revealed that near-field coupling effects between different layers of the array become increasingly important when immersed in a higher refractive index medium [19]. We see this as another potentially fruitful area for future LILAC studies, since it is relatively easy to control the number of colloidal layers using spin coating techniques or a bimodal colloidal crystal template.

Conclusions

Laser-initiated, liquid-assisted colloidal lithography has been used to form 3-D patterns on silicon substrates. The technique combines single shot ~50 fs laser pulses, together with self-assembled arrays of colloidal particles on the Si substrates immersed in different refractive index liquid media to tune the optical near-field effects around the colloidal particles. We demonstrate formation of extended arrays of bumps (with base diameter ~1.3 μm and height ~100 nm) when using a monolayer of silica colloidal particles with R = 1.5 μm immersed in methanol, acetonitrile or n-hexane (*i.e*. liquids with $n_{liquid} < n_{colloid}$). Use of liquids with $n_{liquid} > n_{colloid}$ (*e.g*. chloroform, carbon tetrachloride or toluene), in contrast, yields a repeat pattern comprising both holes (with width ~400 nm and depth ~100 nm) and bumps (which are also ~400 nm in diameter at their base). The different surface patterns accord with the results of Mie scattering simulations, which show that the near field enhancement effects are sensitively dependent upon the difference in the refractive index of the liquid medium and the colloidal particle. The simulations also indicate a significant increase in the depth of focus when using a liquid medium to assist the laser processing, which has also been confirmed experimentally by 3-D patterning a Si substrate surface by LILAC lithography through a double layer of hexagonally close packed silica colloidal particles.

Acknowledgments: MU and MPG acknowledge financial support through Marie Curie Intra-European and International Incoming Fellowships (FP7-PEOPLE-2013-IEF-625403, and PIIF-GA-2012-326988, respectively). The authors are also grateful to Prof. A.J. Orr-Ewing for access to a fs laser system acquired via ERC Advanced Grant 290966 CAPRI, to Dr. T. Sjostrom for use of an O_2 plasma etcher, to J.A. Jones for assistance with the SEM measurements and to Drs W.H. Briscoe and B.S. Truscott for many helpful discussions.

References

[1] R. S. Dhaliwal, W. A. Enichen, S. D. M. S. Gordon, R. A. Kendall, J. E. Lieberman, H. C. Pfeiffer, D. J. Pinckney, C. F. Robinson, J. D. Rockrohr, W. Stickel, E. V. Tressler, IBM J. Res. Dev. (2001) 45, 615-638 doi: 10.1147/rd.455.0615

[2] R. D. Piner, J. Zhu, F. Xu, S. Hong and C. A. Mirkin, Science (1999) 283, 661-663 doi: 10.1126/science.283.5402.661

[3] D. G. Georgiev, R. J. Baird, I. Avrutsky, G. Auner and G. Newaz, Appl. Phys. Lett. (2004) 84, 4881-4883 doi: 10.1063/1.1762978

[4] K. Piglmayer, R. Denk and D. Bauerle, Appl. Phys. Lett. (2002) 80, 4693-4695 doi: 10.1063/1.1489085

[5] Z. B. Wang, W. Guo, A. Pena, D. Whitehead, B. S. Lukyanchuk, L. Lin, Z. Liu, Y. Zhou and M. H. Hong, Opt. Express (2008) 16, 19706-19711 doi: 10.1364/OE.16.019706

[6] M. Ulmeanu, P Petkov, H Hirshy and E Brousseau, Mater. Res. Express (2014) 1, 015030-9 doi:10.1088/2053-1591/1/1/015030

[7] J. P. Moening and D. G. Georgiev, J. Appl. Phys. (2010) 107, 014307-5 doi: 10.1063/1.3273489

[8] R. Piparia, E. W. Rothe and R. J. Baird, Appl. Phys. Lett. (2006) 89, 223113-3 doi: 10.1063/1.2397569

[9] R. L. Smith and S. D. Collins, J. Appl. Phys. (1992) 71, R1-22 doi: 10.1063/1.350839

[10] Z. Wang, N. T. Nguyen, W. A. H. Wien, H. Schellevis, P. M. Sarro and J. N. Burghartz, IEEE Transactions on Advanced Packaging (2006) 29, 615-622 doi: 10.1109/TADVP.2005.853552

[11] M. Ulmeanu, L. E. Sima, D. Ursescu, M. Enculescu, X. Bazan and I. Quintana, Current Topics in Medicinal Chemistry (2014) 14, 624-629 doi: 10.2174/1568026614666140118204946

[12] G. Mie, Annalen der Physik (1908) 330, 377-445 doi: 10.1002/andp.19083300302

[13] The Mie theory, Basics and Applications, Springer Series in Optical Sciences (2012), W. Hergert and T. Wriedt (Eds.) ISBN: 978-3-642-28737-4

[14] Handbook of Optical Constants of Solids, Academic Press (1988), E. D. Palik (Ed.) ISBN: 0-12-544423-0

[15] L. Berthe, R. Fabbro, P. Peyre, L. Tollier and E. Bartnicki, J. Appl. Phys. (1997) 82, 2826–2832 doi: 10.1063/1.366113

[16] Laser Cleaning, World Scientific (2002), B. Luk'yanchuk (Ed.) ISBN 981-02-4941-1

[17] S.M. Huang, Z. Sun, B.S. Luk'yanchuk, M.H. Hong and L.P. Shi, Appl. Phys. Lett. (2005) 86, 161911-3 doi: 10.1063/1.1886896

[18] S.M. Huang, Z. Sun and Y.F. Lu, Nanotechnology (2007) 18, 025302-7 doi:10.1088/0957-4484/18/2/025302

[19] Z.B. Wang, W. Guo, B. Luk'yanchuk, D.J. Whitehead, L. Li and Z. Liu, J. Laser Micro/Nanoeng. (2008) 3, 14–18 doi: 10.2961/jlmn.2008.01.0004